PHYSICAL REVIEW A VOLUME 13, NUMBER 3 MARCH 1976

Study of the L-shell x rays of Ta, Pt, Au, Hg, and Pb by proton bombardment*

James R. Chen, Jerry D. Reber, David J. Ellis, and Thomas E. Miller
Department of Physics, State University of New York, College at Geneseo, Geneseo, New York 14454
(Received 16 September 1975; revised manuscript received 10 November 1975)

The L x-ray transition ratios $L(\alpha_{12}/l)$, $L(\gamma_1/\eta)$, $L(\eta/\gamma_5)$, $L(\gamma_{236}/\gamma_1)$, and $L(\gamma_{44'}/\gamma_1)$ have been measured for the elements ^{73}Ta, ^{78}Pt, ^{79}Au, ^{80}Hg, and ^{82}Pb by ionization of the L-subshell electrons with 0.4–2.0-MeV proton bombardment. Transition-rate ratios $L(\gamma_{23}/\gamma_{44'})$ to the L_1 subshell, $L(\gamma_6/\gamma_1)$, $L(\gamma_1/\eta)$, and $L(\eta/\gamma_5)$ to the L_2 subshell, and $L(\alpha_{12}/l)$ to the L_3 subshell have been extracted. Comparison of the extracted ratios with the relativistic Hartree-Fock model calculations of Scofield shows agreement within experimental errors for the L_1, L_2, and L_3 subshell ratios. A previously reported minimum in the Pb $L(\alpha_{12}/l)$ ratio between proton energies 1.0 to 1.5 MeV was not observed. Total L-shell production cross sections have also been measured for Pt and Au over the energy range 0.4–2.0 MeV and are found to be in good agreement with the predictions of the nonrelativistic plane-wave Born approximation and the constrained binary-encounter approximation, but not with the binary-encounter approximation.

I. INTRODUCTION

With the continued advance of experimental and theoretical techniques more refined types of experiments in atomic and nuclear physics have become feasible. In particular, considerable effort in recent years has gone into the understanding of inner-shell ionization by ion bombardment.[1] Recent calculations of K- and L-subshell transition rates have been obtained by Scofield[2,3] using separate relativistic Hartree-Fock wave functions for the initial and final states of the atom. In this work we have extracted ratios of specific transition rates to the L_1, L_2, and L_3 subshells in Ta, Pt, Au, Hg, and Pb using a high-resolution Si(Li) x-ray detector.

The creation of inner-shell atomic vacancies may be accomplished by radioactive decay,[4] x-ray fluorescence,[5] or charged-particle-induced emission with electrons,[6] protons,[7–11] or alpha[9,12] particles. The subsequent L x-ray transitions refer to x rays emitted during the transition of an electron from an allowed energy level to either the $2s_{1/2}$, $2p_{1/2}$, or $2p_{3/2}$ vacant level, labeled L_1, L_2, and L_3 transitions respectively (Fig. 1). The ratio of two transition rates to the same L subshell e.g., $L_1(\gamma_{23}/\gamma_{44'})$,[13] $L_2(\gamma_1/\eta)$, $L_3(\alpha_{12}/l)$, etc., is expected to be independent of ion bombardment energy.[3] Several recent measurements of $L_3(\alpha_{12}/l)$ by radioactive decay,[4] by electron[6] and proton[7] bombardment have found disagreements with Scofield's calculations. The electron and source measurements are higher while the proton measurements of Ref. 11 are lower than predicted. Busch *et al.*[7] have observed a minimum in the Pb $L_3(\alpha_{12}/l)$ ratio for incident proton energies between $E_p = 1.0–1.5$ MeV.

In this paper we report transition rate ratios for $L_1(\gamma_{23}/\gamma_{44'})$, $L_2(\gamma_6/\gamma_1)$, $L_2(\gamma_1/\eta)$, $L_2(\eta/\gamma_5)$, and $L_3(\alpha_{12}/l)$ for the elements Ta, Pt, Au, Hg, and Pb for proton energies ranging from 0.4 to 2.0 MeV.

Total L-shell production cross sections have also been studied by several authors.[7,11,14] We report total L-shell cross sections for Pt and Au over the energy range 0.4 to 2.0 MeV and compare the data with the predictions of the nonrelativistic plane-wave Born approximation (PWBA),[15] the constrained binary-encounter approximation

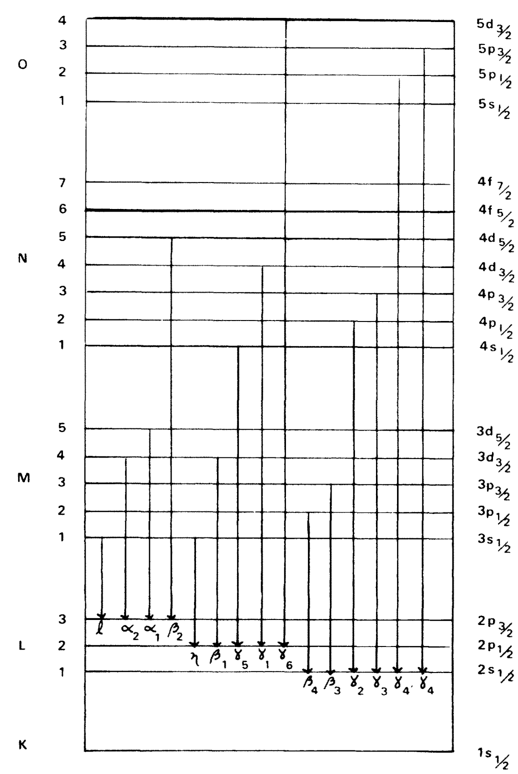

FIG. 1. Schematic diagram for L x-ray transitions. Only the major transitions studied are shown. Energy levels are not to scale.

(CBEA),[16] and the binary-encounter approximation (BEA).[17]

II. EXPERIMENTAL METHOD

A 5–50 nA beam of protons from a 2-MeV Van de Graaff accelerator was collimated by two graphite collimators to produce a circular 0.32-cm-diam beam spot at the target. The targets of Ta, Pt, Au, Hg_2F_2, and Pb were 50–100 $\mu g/cm^2$ thick deposited on 20-$\mu g/cm^2$ carbon backings and were mounted in aluminum frames at 45° to the incident beam. The thickness of the target foils was chosen to minimize proton energy loss and self-absorption of the x rays in the target.

The characteristic L x rays were detected using a Si(Li) detector with a full width at half-maximum resolution of 165 eV at 5.9 keV. The detector was located directly below the target at 90° to the incident beam and was mounted inside the vacuum system of the target chamber. A 0.025-cm Mylar attenuator was placed before the detector to attenuate the copious M x rays. Hence the L x rays from the target were required to pass through a 0.025-cm Mylar attenuator and a 0.0025-cm Be detector window. The absolute efficiency of the detector system, which includes the intrinsic efficiency and fractional solid angle intercepted by the Si(Li) detector as well as the x-ray attenuation by the Mylar and Be window, was measured using calibrated radioactive sources of ^{54}Mn, ^{57}Co, ^{65}Zn, and ^{241}Am following established procedures.[18]

The targets were bombarded from 30 to 90 min. each at an x-ray count rate of approximately 300 counts/sec. Generally, data were acquired until the counts in the weak $L\gamma_{44'}$ peak were 200 counts or more. Dead-time corrections were less than a few percent. The data were converted to digital format for later analysis on a CDC 6400 computer.

The incident beam intensity was monitored by a Faraday cup and the information used in the calculation of the total cross sections. In addition a Si surface barrier detector mounted directly above the target at 90° to the incident beam continuously monitored the elastically scattered protons. The yield of elastically scattered protons was observed at all incident energies to check the agreement with the Rutherford scattering cross-section predictions. These measurements showed agreement with the E^{-2} dependence of the Rutherford predictions within the $\leq 2\%$ statistical uncertainty of the measurements.

III. DATA ANALYSIS

With the resolution achieved, the L x-ray spectrum can be subdivided into three main groups: the $L\alpha_{12}$ group with the weaker Ll and $L\eta$ lines in the tails; the $L\beta$ group; and the $L\gamma$ group (Fig. 2). The Ll, $L\alpha_{12}$, and $L\eta$ lines were fitted using single Gaussians. The $L\beta$ group could not be separated into distinct transitions, owing to the large number of contributing transitions to the $L\beta$ group of lines. The $L\gamma$ lines were decomposed into four Gaussians and the constituents identified as $L\gamma_5$, $L\gamma_1$, $L\gamma_{236}$, and $L\gamma_{44'}$. Figure 3 shows the decomposition of the Au $L\gamma$ lines for a proton energy of 0.4 MeV.

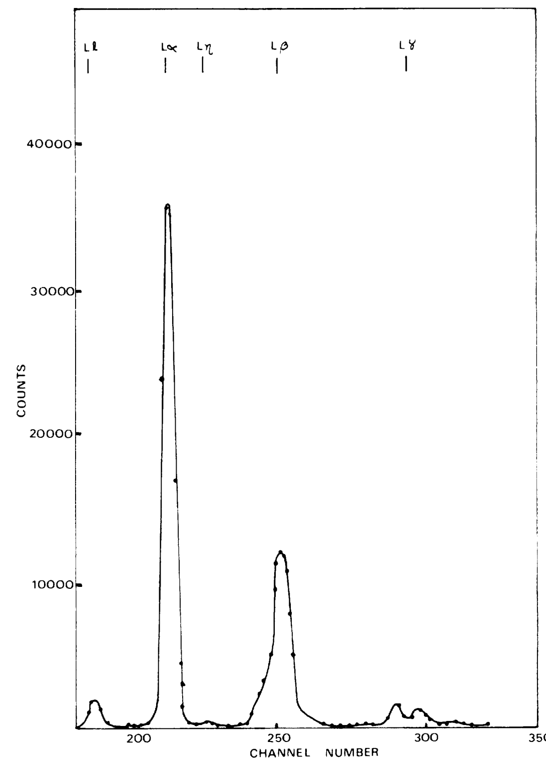

FIG. 2. Pulse-height spectrum for 0.4-MeV protons on Au.

Decomposition of the various peaks as well as the determination of the intensities of single lines were made using an interactive data analysis program.[19] The decomposition of multiple lines was performed using an interactive least-squares-fitting algorithm due to Bevington.[20]

IV. RESULTS AND DISCUSSION

A. Total cross sections

Total L-shell production cross sections for Pt and Au are shown in Figs. 4 and 5, respectively, together with the predictions of the PWBA, CBEA, and BEA model calculations. The measurements in the laboratory give x-ray production cross sections [$\sigma_T(L$ x ray)], which are related to the calculated ionization cross sections σ_T(ionization) by

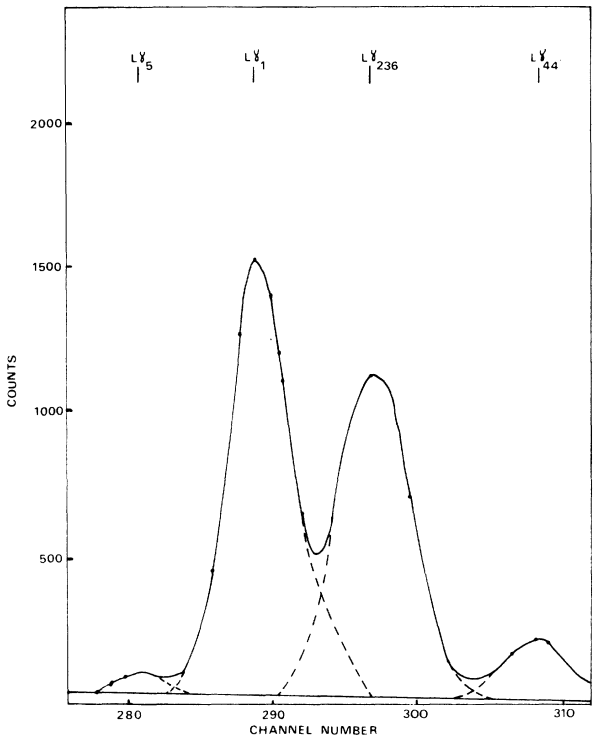

FIG. 3. Decomposition of the $L\gamma$ lines for 0.4-MeV protons on Au.

$\sigma_T(L \text{ x ray}) = \omega_L \sigma_T(\text{ionization})$. ω_L is the average L-shell fluorescence yield, taken from Bambynek *et al.*[21] As can be seen from Figs. 4 and 5 the PWBA and the CBEA predict almost identical theoretical values for both Pt and Au above 1 MeV, but below 1 MeV the CBEA drops below the PWBA. However, both the PWBA and CBEA agree with the measured cross sections within the error bars of the data. The BEA predicts the general shape of the experimental data, but is consistently lower than the data.

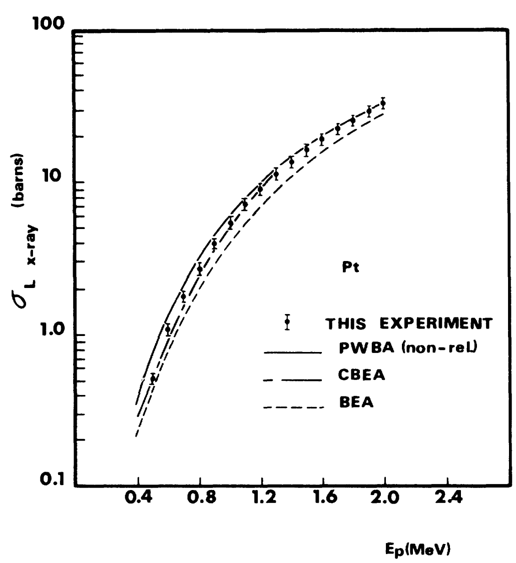

FIG. 4. Measured values of total L-shell production cross section for Pt compared with the predictions of the PWBA, CBEA, and BEA.

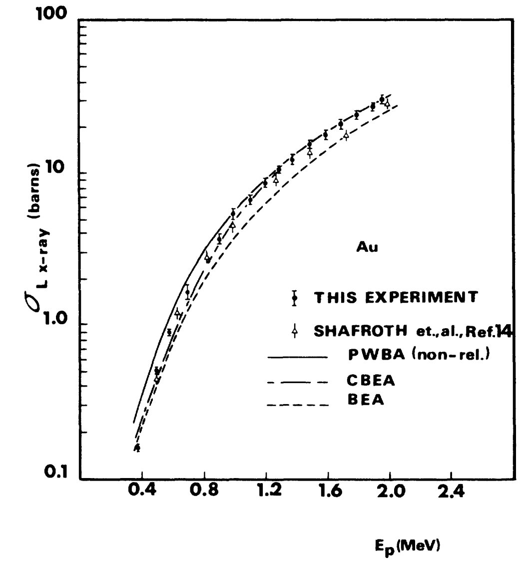

FIG. 5. Measured values of total L-shell production cross section for Au compared with the predictions of the PWBA, CBEA, and BEA. The data of Shafroth *et al* (Ref. 14) is also shown.

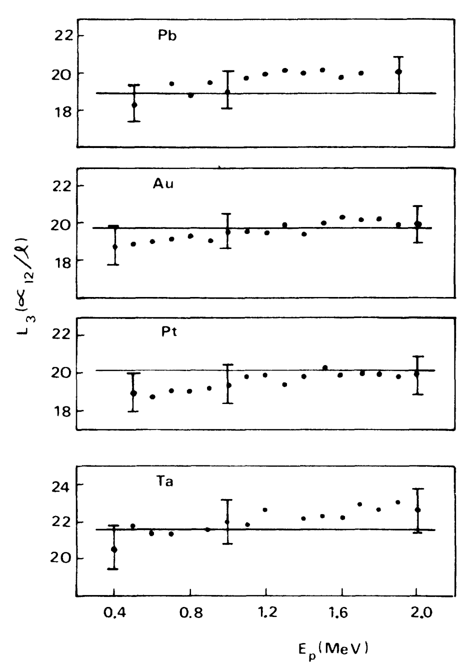

FIG. 6. Measured values of $L_3(\alpha_{12}/l)$ ratios (●) compared with the predicted radiative-width ratios $\Gamma_{\alpha_{1,2}}/\Gamma_l$ (solid lines) of Scofield (Ref. 3).

TABLE I. $L_3(\alpha_{12}/l)$ ratios.

Element	Radioactive decay (Ref. 4)	X-ray fluorescence (Ref. 5)	α-particle bombardment (Ref. 12)	Electron bombardment (Ref. 6)	Proton bombardment	Theory (Ref. 3)
^{82}Pb	20.1±1.0	18.2 ±1.7	19.4±1.3	···	19.7±1.0 [a] Minimum in data [c] at E_p = 1–1.5 MeV	18.95
^{79}Au	···	18.72±1.2	···	25.25	19.7±1.0 [a]	19.8
^{78}Pt	···	···	···	···	19.6±1.0 [a]	20.2
^{73}Ta	23.7±1.0	19.6 ±2.0	21.7±1.7	26.39(19.4) [b]	22.1±1.2 [a]	21.62
^{66}Dy	···	···	···	···	19.0±2.7 [d]	23.6
^{65}Tb	26.1±1.5	···	···	37.88(21.4)	···	23.9

[a] This experiment.
[b] Only the $L_3(\alpha_1/l)$ ratio was available; values in parentheses are the theoretical values of Ref. 3.
[c] Reference 7.
[d] Average of data reported, Ref. 11.

Also shown in Fig. 5 are the data of Shafroth *et al.*[14] The agreement between the data of this experiment and those of Shafroth *et al.* is within the reported uncertainties over the entire energy range studied.

B. L_3 subshell ratio

The $L\alpha_{12}$ and Ll transitions arise from L_3 subshell vacancy fillings. Figure 6 shows the ratio $L_3(\alpha_{12}/l)$ for the various elements together with the relativistic Hartree-Fock model predictions.[3] The agreement between the data and theory is within the experimental uncertainties for all elements studied. Busch *et al.*[7] reported a minimum in the Pb data between E_p = 1.0–1.5 MeV. The Pb data reported here are consistent with a constant value for this ratio.

Table I lists the measured $L_3(\alpha_{12}/l)$ ratios for various elements using different methods of creating the L_3 subshell vacancy, as well as the calculations by Scofield.

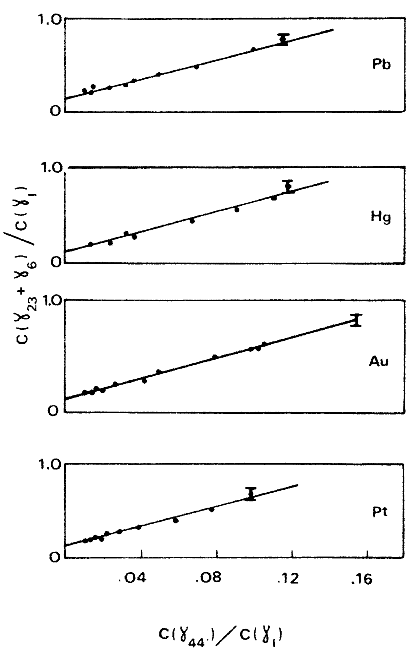

FIG. 7. Plot of $C(\gamma_{23}+\gamma_6)/C(\gamma_1)$ vs $C(\gamma_{44'})/C(\gamma_1)$. The lines shown are the least-squares-fits to the experimental data points. Intercepts are listed in Table II and compared with the predictions of Scofield (see text).

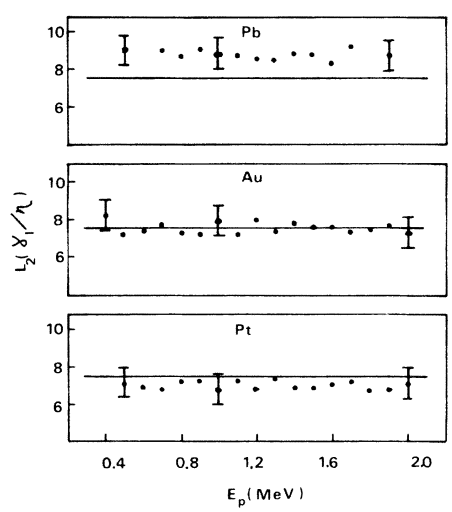

FIG. 8. Measured values of $L_2(\gamma_1/\eta)$ ratios (•) compared with the predicted radiative-width ratios $\Gamma_{\gamma_1}/\Gamma_\eta$ (solid lines) of Scofield (Ref. 3).

TABLE II. $L_2(\gamma_6/\gamma_1)$ ratios.

Element	This experiment	Other measurements	Theory (Ref. 3)
^{78}Pt	0.126 ± 0.013		0.093
^{79}Au	0.128 ± 0.013	0.11 (Ref. 22) 0.125 ± 0.01 (Ref. 8)	0.105
^{80}Hg	0.139 ± 0.020		0.116
^{82}Pb	0.153 ± 0.015		0.135

C. L_2 subshell ratio

The $L\gamma$ group of lines contains contributions from the $L_2(\gamma_1, \gamma_5,$ and $\gamma_6)$ subshell transitions and the $L_1(\gamma_{23}$ and $\gamma_{44'})$ subshell transitions. The γ_2, γ_3, and γ_6 lines were unresolvable; for example in Pb the γ_2, γ_3, and γ_6 lines occur at 15.097, 15.218, and 15.180 keV, respectively. In order to determine the relative transition ratio $L_2(\gamma_6/\gamma_1)$, use was made of the significant energy variation in the counts $C(\gamma_{23}+\gamma_6)$, $C(\gamma_1)$, and $C(\gamma_{44'})$ in the respective photopeaks. Using the relation

$$C(\gamma_{23}+\gamma_6) = (\tau_{\gamma_6}/\tau_{\gamma_1})C(\gamma_1) + (\tau_{\gamma_{23}}/\tau_{\gamma_{44'}})C(\gamma_{44'}),$$

where $\tau_{\gamma_6}/\tau_{\gamma_1}$ is the relative transition probabilities for the γ_6 to γ_1 lines, a plot of $C(\gamma_{23}+\gamma_6)/C(\gamma_1)$ versus $C(\gamma_{44'})/C(\gamma_1)$ was made for the various elements (Fig. 7). Table II lists the resulting intercepts as well as the theoretical calculations of Scofield. The agreement is within 1–2 standard deviations and within 2.5σ for Pt.

Figure 8 shows the $L_2(\gamma_1/\eta)$ and Fig. 9 shows the $L_2(\eta/\gamma_5)$ ratios with the theoretical calculations. The agreement is good for Au and within 1.5σ for Pb.

D. L_1 subshell ratios

A determination of the $L_1(\gamma_{23}/\gamma_{44'})$ ratio can be obtained from the slopes of the plots in Fig. 7.

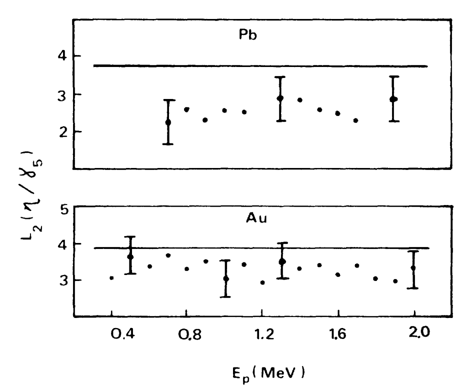

FIG. 9. Measured values of $L_2(\eta/\gamma_5)$ ratios (●) compared with the predicted radiative-width ratios $\Gamma_\eta/\Gamma_{\gamma_5}$ (solid lines) of Scofield (Ref. 3).

Table III lists the resulting slopes as well as the relativistic Hartree-Fock model predictions. The agreement with the corrected[3] Scofield calculations is excellent.

V. CONCLUSIONS

Total L-shell production cross sections for Pt and Au are in good agreement with the predictions of the PWBA and the CBEA over the energy range 0.4 to 2.0 MeV. The BEA predicts the general shape but is consistently lower than the experimental data.

There is agreement within experimental uncertainties between the measured L_1, L_2, and L_3 subshell transition rate ratios $L_1(\gamma_{23}/\gamma_{44'})$, $L_2(\gamma_6/\gamma_1)$, $L_2(\gamma_1/\eta)$, $L_2(\eta/\gamma_5)$, and $L_3(\alpha_{12}/l)$, with the relativistic Hartree-Fock model calculations of Scofield.

For the $L_3(\alpha_{12}/l)$ ratio, this conclusion agrees with the available measurements using x-ray fluorescence, α particle, and some proton bombardment, but not with the measurements using radioactive decays and electron bombardment. The reported minimum in the Pb ratio at proton energies betweeen 1.0–1.5 MeV was not observed.

ACKNOWLEDGMENTS

We would like to express our appreciation to T. A. Cahill and R. A. Eldred for the use of the computer analysis codes, and to P. W. Alley, L. T. Bryant, R. P. Coco, and K. F. Kinsey for their assistance with the data analysis programs. Many fruitful discussions with T. J. Gray and R. L. Sells are also greatly acknowledged.

TABLE III. $L_1(\gamma_{23}/\gamma_{11'})$ ratios.

Element	This expt.	Theory (Ref. 3)
^{78}Pt	5.34 ± 0.5	5.78
^{79}Au	5.51 ± 0.5	5.60
^{80}Hg	5.38 ± 0.5	5.42
^{82}Pb	5.11 ± 0.5	5.08

*Work supported in part by grants from the Research Foundation of SUNY.

[1] *Proceedings of the International Conference on Inner Shell Ionization Phenomena and Future Applications, Atlanta, Georgia, 1972,* edited by R. W. Fink, S. T. Manson, J. M. Palms, and P. V. Rao (U.S. AEC, Oak Ridge, Tenn., 1973).

[2] J. H. Scofield, Phys. Rev. A 9, 1041 (1974).

[3] J. H. Scofield, Phys. Rev. A 10, 1507 (1974); errata, Phys. Rev. A 12, 345 (1975).

[4] D. W. Nix, J. C. McGeorge, and R. W. Fink, Phys. Lett. 46A, 205 (1973).

[5] J. H. McCrary, L. V. Singman, L. H. Ziegler, L. O. Loomey, C. M. Edmonds, and C. E. Harris, Phys. Rev. A 5, 1587 (1972).

[6] S. I. Salem, D. C. Clark, and R. T. Tsutsui, Phys. Rev. A 5, 2390 (1972); S. I. Salem, R. T. Tsutsui, and B. A. Rabbini, Phys. Rev. A 4, 1728 (1971).

[7] C. E. Busch, A. B. Baskin, P. H. Nettles, S. M. Shafroth, and A. W. Wattner, Phys. Rev. A 7, 1601 (1973).

[8] S. Datz, J. L. Duggan, L. C. Feldman, E. Laegsgaard, and J. U. Andersen, Phys. Rev. A 9, 192 (1974).

[9] C. N. Chang, J. F. Morgan, and S. L. Blatt, Phys. Rev. A 11, 607 (1975).

[10] D. H. Madison, A. B. Baskin, C. E. Busch, and S. M. Shafroth, Phys. Rev. A 9, 675 (1974).

[11] F. Abrath and T. J. Gray, Phys. Rev. A 10, 1157 (1974).

[12] R. K. Wyrick and T. A. Cahill, Phys. Rev. A 8, 2288 (1973).

[13] The symbol $L_1(\gamma_{23}/\gamma_{44'})$ means $[L(\gamma_2)+L(\gamma_3)]/[L(\gamma_4)+L(\gamma_{4'})]$. The subscript 1 indicates that all the transitions are to the L_1 subshell.

[14] S. M. Shafroth, G. A. Bissinger, and A. W. Wattner, Phys. Rev. A 7, 566 (1973).

[15] B.-H. Choi, E. Merzbacher, and G. S. Khandewal, At. Data 5, 291 (1973).

[16] J. S. Hansen, Phys. Rev. A 8, 822 (1973).

[17] J. D. Garcia, E. Gerjuoy, and J. E. Welker, Phys. Rev. 165, 66 (1967).

[18] L. B. Magnusson, Phys. Rev. 107, 161 (1957); J. S. Hansen, J. C. McGeorge, D. Nix, W. D. Schmidt-Ott, I. Unus, and R. W. Fink, Nucl. Instrum. Methods 106, 365 (1973); R. J. Gehrke and R. A. Lokken, Nucl. Instrum. Methods 97, 219 (1971).

[19] J. F. Harrison and R. A. Eldred, *Advances in X-Ray Analysis* (Plenum, New York, 1973), Vol. 17, pp. 560–570.

[20] P. Bevington, *Data Reduction and Error Analysis for Physical Science* (McGraw-Hill, New York, 1969).

[21] W. Bambynek, B. Craseman, R. W. Fink, H. V. Freund, H. Mark, C. D. Swift, R. E. Price, and P. Venugopala Rao, Rev. Mod. Phys. 44, 716 (1972).

[22] J. N. Cooper, Phys. Rev. 61, 234 (1942).